Supplementary Information

Enhancing CO_2 Photocatalytic Reduction with a Novel Polymer Catalyst: Inducing Reactive C–N Bond Formation Through Altered Thermodynamic Trends and Exploring Reduction Kinetics

Xiaofang Shang[a], Zheng Lian[a], Jiaqi Li[a], Jie Ding[a], Qin Zhong[a]**

[a]School of Chemistry and Chemical Engineering, Nanjing University of Science and Technology, Nanjing, Jiangsu Province, 210094, PR China

* Corresponding author, Tel.: +86 25 84303232, fax: +86 25 84315134

* E-mail: tonlyjding@njust.edu.cn (Jie Ding); zq304@njust.edu.cn (Qin Zhong)

Contents

1. Experimental Section/Methods

1.1. Materials:

Melamine, resorcinol, formaldehyde, Sodium carbonate were purchased from Aladdin Co., Ltd. The above reagents were all of analytical grade and used without further purification.

1.2. Synthesis of samples:

Materials:

Melamine, resorcinol, formaldehyde and sodium carbonate were purchased from Aladdin Co., Ltd. The above reagents were all of analytical grade and used without further purification.

Preparation of melamine-formaldehyde-resorcinol polymer

Melamine-Formaldehyde-Resorcinol (M) were synthesized via a hydrothermal method:

1. Place 0.77 g of resorcinol and 1.15 g of formaldehyde into a 50 mL beaker. 6 mL water was used as the solvent, and the mixture was continuously stirred for 1 hour at 40 ℃ to obtain 2,4-dihydroxymethyl-1,3-diphenol.

2. Subsequently, dissolve 0.90 g of melamine and 1.70 g of formaldehyde in another 6 mL of distilled water in another beaker at 80 °C until the solution becomes clear to obtain 2,4,6-trimethylamino-1,3,5-triazine.

3. Then, mix the above two solutions and stir continuously for 0.5 hours at 40 ℃. Place the mixture into a Teflon-lined autoclave and heat it for 24 hours at 120 °C under constant stirring conditions.

4. Finally, recover the product by repeated washing (5 times) and air-drying for 24 hours at 100 °C.

5. Calcined at 120 ºC for 4h under nitrogen atmosphere.

Additionally, the polymerization process was presented in Figure S1.

Preparation of X NaM

X NaM, where X was the mass percentage of Na_2CO_3 (X= 10, 15, 20 mg).

1. Place 0.77 g of resorcinol, 1.15 g of formaldehyde and Na_2CO_3 into a 50 mL beaker. 6 mL water was used as the solvent, and the mixture was continuously stirred for 1 hour at 40 ℃.

2. Subsequently, dissolve 0.90 g of melamine and 1.70 g of formaldehyde in another 6 mL of distilled water in another beaker at 80 °C until the solution becomes clear to obtain 2,4,6-trimethylamino-1,3,5-triazine.

3. Then, mix the above two solutions and stir continuously for 0.5 hours at 40 ℃. Place the mixture into a Teflon-lined autoclave and heat it for 24 hours at 120 °C under constant stirring conditions.

4. Finally, recover the product by repeated washing (5 times) and air-drying for 24 hours at 100 °C.

5. Calcined at 120 ℃ for 4h under nitrogen atmosphere.

1.3. Catalyst characterization

The catalyst's morphology and structure were analyzed using various techniques, including X-ray diffraction (XRD) with Cu Kα radiation, scanning electron microscopy (SEM), Fourier transform infrared (FT-IR) spectroscopy, and 13C solid-state nuclear magnetic resonance (SSNMR). Furthermore, CO_2 pulse adsorption test was conducted on a Micromeritics AutoChem II 2920 chemisorption analyzer equipped with a thermal conductivity detector (TCD), and mass spectroscopy (MS) was performed using a TPR-20 EGA (Hiden Analytical) spectrometer. The morphology was investigated using field emission scanning transmission microscopy (SEM, Regulus-8100, HITACHI, Japan)。 UV-VIS-NIR diffuse reflectance (UV-VIS-NIR DRS) was characterized through a Shimadzu UV-2600 UV-vis spectrophotometer. Electrochemistry impedance spectroscopy (EIS), transient photocurrent responses, and Mott-Schottky analysis were carried out using an electrochemical workstation (CHI760D) with a three-electrode configuration, including working electrode, Pt electrode, and Ag/AgCl as the reference electrode. Additionally, X-ray photoelectron spectroscopy (XPS) tests of the catalysts were performed on a Thermo ESCALAB 250 spectrometer (Thermo Scientific), and the Brunauer-Emmett-Teller (BET) specific surface area was calculated using a Micro ASAP 2460 with nitrogen adsorption at 77 K. In-situ FT-IR experiments were conducted using a Thermo Fisher Nicolet iS20 spectrometer, which was equipped with a liquid-nitrogen-cooled MCT detector. Each spectrum was generated from 32 scans averaged at a resolution of 4 cm^{-1}. Prior to the experiments, we obtained the background spectrum by purging the catalysts at 120 °C in an N_2 atmosphere (40 mL/min) for 90

minutes and then cooling to 60 °C. Subsequently, the reaction was initiated in darkness by introducing CO_2 (20 mL/min) bubbled with H_2O into the in-situ tank for 60 minutes to achieve adsorption-desorption equilibrium, and the resulting intermediates were monitored. Following this, the light source was activated, and the resulting intermediates were observed for the next 60 minutes. In addition, in situ CO_2 adsorption experiments were performed in the dark without H_2O.

1.4. Calculation process of CO production rates:

At the outset, a gas chromatograph was utilized to detect and quantify 0.5 mL of a calibration gas containing 0.505% CO. The online analysis generated an area value labeled as 0.505% CO. Subsequently, 0.5 mL of the gas produced during the photocatalytic reaction was introduced into a gas chromatograph to obtain another area designated as A 0.5mL CO. To calculate the CO production rates, the following expression can be used:

$$Yield = \frac{P_{CO} * V_{CO} * n_0 * \ 0.505\%}{P_0 * A_{0.505\%} * T * m} \quad (1)$$

Where "P_{CO}" represents the pressure at the outlet; "V_{CO}" signifies the volume (based on a 0.5 mL injection gas volume with adjustments considering the scaling factor of the reactor); "n_0" stands for the total number of molecules in 0.5 mL of gas; "P_0" denotes standard atmospheric pressure; "T" indicates the reaction time; and "m" refers to the dosage of catalysts.

1.5. Calculation process of CH_3OH production rates:

The production rates of CH_3OH are obtained by the same methods by using 0.0992% CH_3OH as calibrating gas, as described in Eqs. (2):

$$Yield = \frac{P_{CH3OH} * V_{CH3OH} * n_0 * \ 0.0992\%}{P_0 * A_{0.0992\%} * T * m} \tag{2}$$

Where "V_{CH3OH}" denotes the volume of the autoclave (based on a 0.5 ml injection gas volume with adjustments considering the scaling factor of the reactor); "n_0" signifies the 0.5 mL of gas; "P_0" indicates standard atmospheric pressure; "T" refers to the reaction time, and "m" represents the dosages of catalysts.

1.6. Labeled $H_2{}^{18}O$ and $^{13}CO_2$ experiments:

$H_2{}^{18}O$ labeling experiment was conducted to confirm the oxygen source of O_2, 30 mg of catalyst and 1mL of $H_2{}^{18}O$ were placed in the reactor, vacuumed to remove the original gas, and then the reactor was continuously inflated with CO_2 (99.9999%) for 3 times to completely remove the air interference. After the final evacuation, the reactor was filled with 0.5 MPa of CO_2 and sealed. The photocatalytic labeled experiment was then conducted by irradiating the mixture for 4 hours. Gas samples from the reactor were collected and analyzed by using a mass spectrometry (Hiden).

To confirm the carbon source of CH_3OH in this work, the $^{13}CO_2$-labeled experiment was carried out. Following the addition of 30 mg catalyst and 1 mL H_2O into the reactor, the mixture was stirred, and $^{13}CO_2$ was introduced to achieve a gas pressure of 0.50 MPa. The reactor was then evacuated, and this filled-pump cycle was repeated three times. Upon the final evacuation, the reactor was filled with 0.5 MPa of $^{13}CO_2$ and sealed. The photocatalytic labeled experiment was then conducted by irradiating the mixture for 4 hours.

1.7. Calculation method of apparent quantum yield (*AQY* %):

$$AQY_{CH3OH} = \frac{6 * N_a * [CH_3OH]}{I * A * t * \frac{\lambda}{hc}}$$

Where *Na* is Avogadro's number, *[CH_3OH]* is the number of CH_3OH evolved in time "t", *I* is the incident solar irradiance over the exposed area; λ denotes the wavelength (380, 420, 450, and 500nm); *h* is Planck's constant (6.62×10^{-34} J·s), and *c* is the speed of light.

1.8. Calculation process of DFT:

The calculations were performed using the Gaussian 09 package and density functional theory (DFT) [1-2]. MRF and 15 NaM calculation utilized a model comprising 2,4-dihydroxy-1,3-benzenediol and 2,4,6-trimethylamino-1,3,5-triazine. 15 NaM. The specific analogue structures for 15 NaM are N*-C*-N*-C*-N*. The geometric optimization of these models was conducted using the B3LYP with a basis-set combination of 6-31G (d, p) [3-4]. The single point energy was calculated under M062X/def2-TZVP. Solvent effects using the SCRF theory with a continuum solvation model (SMD) [5], in which water as the solvent. Additionally, the DFT-D3 [6] method was employed correct the van der Waals interaction. The free energy values of the structure were obtained by combining the electronic energy with the thermal correction to Gibbs free energy, where the thermal correction to Gibbs free energy is the sum of the zero-point energy (ZPE) and the temperature correction to the Gibbs free energy.

The average local ionization energy is the energy needed to remove an electron from a specific location r within the system. The areas with the lowest values correspond to the electrons that are most weakly bound, highlighting the preferred sites for reactions with electrophiles or radicals. The electrostatic potential at a point around a molecule is typically defined as the work required to move a unit positive charge from infinity to that point. First, the wavefunction of the molecule in its stable configuration is calculated using the Gaussian program. Once the wavefunction is obtained, the electron density at various points in the surrounding space can be determined. The electrostatic potential at each point on selected isodensity surfaces can then be

computed. By combining the electrostatic potential with with the average local ionization energy results, the specific active sites of the catalyst can be identified.

Molecular dynamics evaluating the interaction between 2,4-dihydroxylmethyl-1,3-diphenol and 2,4,6-trimethylamino-1,3,5-triazine at 353 K in a box fulling water is conducted by using CP2K, where the step numbers are 20000 and the initial molecular structure is optimized in Gaussian 09.

1.9. Calculation process of conduction band:

$$E_{NHE} = E_{Ag/AgCl} + E^{\Theta}_{Ag/AgCl} \quad (3)$$

$$E_{CB} = E_{NHE} - 0.2 \quad (4)$$

Where E_{NHE}, $E_{Ag/AgCl}$ and $E^{\Theta}_{Ag/AgCl}$ referred to the converted potential, measured potential and the standard potential (0.1976 V), respectively.

2. Catalyst characterization:

Table S1. Specific surface area, pore volume and pore diameter of M, 10 NaM, 15 NaM and 20 NaM.

Catalyst	[a]Surface area (m^2/g)	pore diameter (nm)	pore volume (cm^3/g)
M	4.24	30.36	0.003
10 NaM	173.73	32.59	0.243
15 NaM	439.85	6.77	0.777
20 NaM	455.04	5.45	0.667

Table S2. Comparison of the photocatalytic activities for CO_2 reduction

Catalyst	CH_3OH Production rate ($\mu mol \cdot g^{-1} h^{-1}$)	Reaction conditions	References
15 NaM	10.11	300 W Xe lamp	this work
$Pb_{0.6}Bi_{1.4}O_2Cl_{1.4}$	6.63	300 W Xe lamp	[7]
S doped C_3N_4	0.37	300 W Xe lamp	[8]
V-$Bi_{19}Br_3S_{27}$	1.6	near-infrared	[9]
Defective g-C_3N_4	3.85	350W Xe lamp (AM1.5 filter)	[10]
TiO_2@$ZnIn_2S_4$	4.13	300 W Xe lamp	[11]
Tube g-C_3N_4	0.88	300 W Xe lamp	[12]
Cubic anatase TiO_2	1.5	350 W Xe lamp equipped with a 420 nm cutoff filter	[13]
Azine-based COFs	0.57	A 500 W Xe lamp with a UV and an IR cutoff filter (800 nm $\geq \lambda \geq$ 420 nm)	[14]
O-g-C_3N_4	0.87	300 W Xe lamp	[15]
Bulk g-C_3N_4	0.17	350 W Xe lamp equipped with a 420 nm cutoff filter	[13]
g-C_3N_4/ZnO	0.6	300 W simulated solar xenon arc lamp	[16]

Table S3. The reaction formula and calculation equation for reaction coordinate analysis in CO_2 reduction to CO and CH_3OH.

Label	Reaction	Free Energy Difference (Δ G)
1	$*+CO_2 \rightarrow *COOH$	$G_{*COOH}- G_{CO2}-G_{*}$
2	$*COOH+H^+ + e^- \rightarrow *CO+H_2O$	$G_{*CO}+G_{H2O}- G_{*COOH}-0.5\ G_{H2}$
3-1	$*CO+H^+ + e^- \rightarrow *+CO$	$G_{*}+G_{CO}-G_{*CO}\ -0.5\ G_{H2}$
3-2	$*CO+H^+ + e^- \rightarrow *CHO$	$G_{*CHO}\ -G_{*CO}\ -0.5\ G_{H2}$
4	$*CHO+H^+ + e^- \rightarrow *CH_2O$	$G_{*CH2O}\ -G_{*CHO}\ -0.5\ G_{H2}$
5	$*CH_2O+H^+ + e^- \rightarrow *CH_2OH$	$G_{*CH2OH}\ -G_{*CH2O}\ -0.5\ G_{H2}$
6	$*CH_2OH+2H^+ + 2e^- \rightarrow CH_3OH+*$	$G_{*}+G_{CH3OH}\ -G_{*CH2OH}\ -\ G_{H2}$

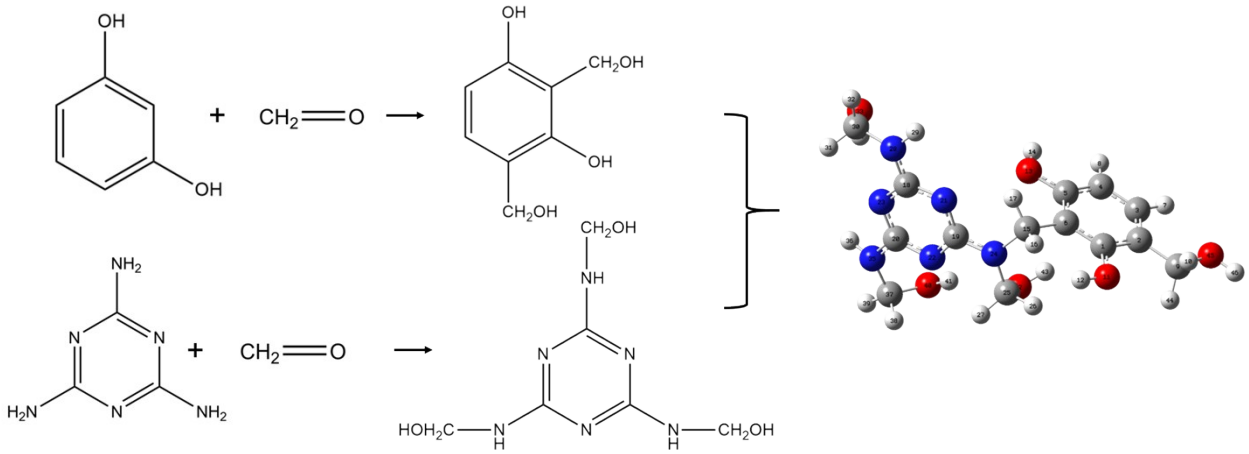

Figure S1. The polymerization process of M.

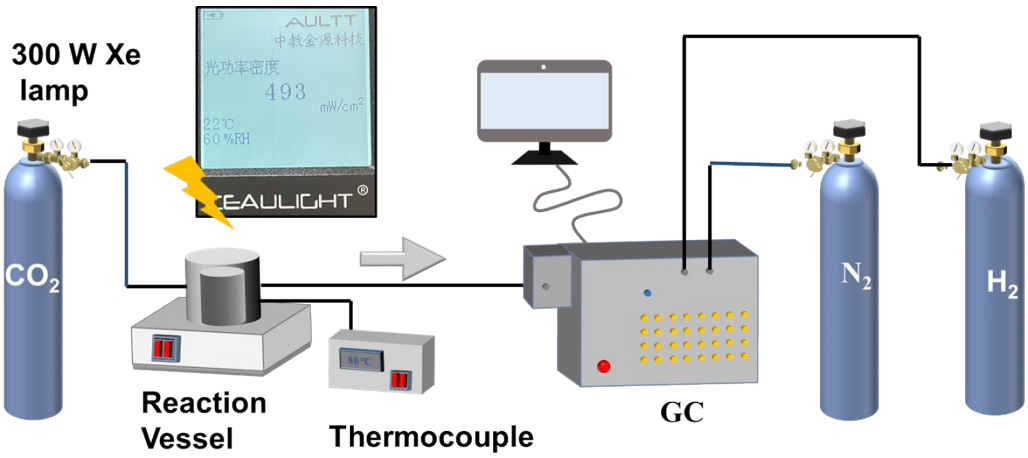

Figure S2. Reaction device for photocatalytic CO_2 to CH_3OH.

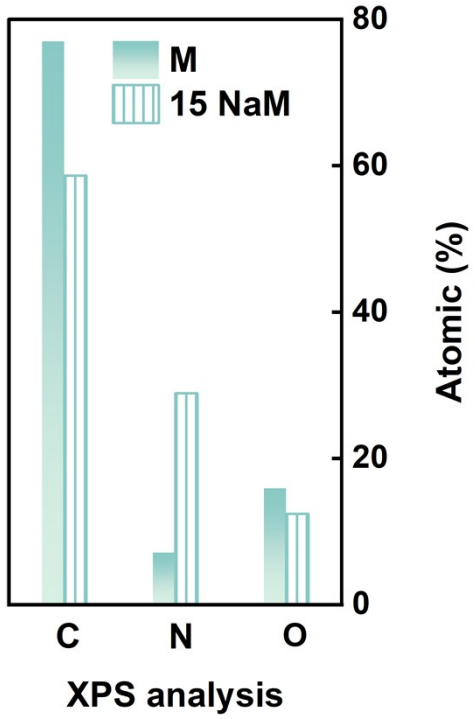

Figure S3. Atomic percentages of M and 15 NaM in XPS patterns.

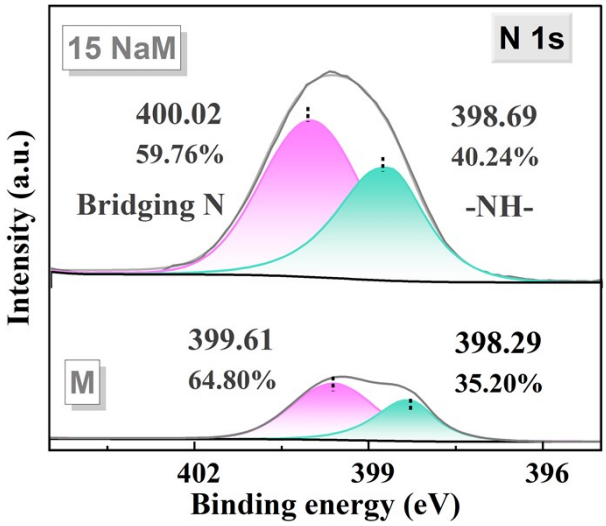

Figure S4. N 1s spectra of M and 15 NaM.

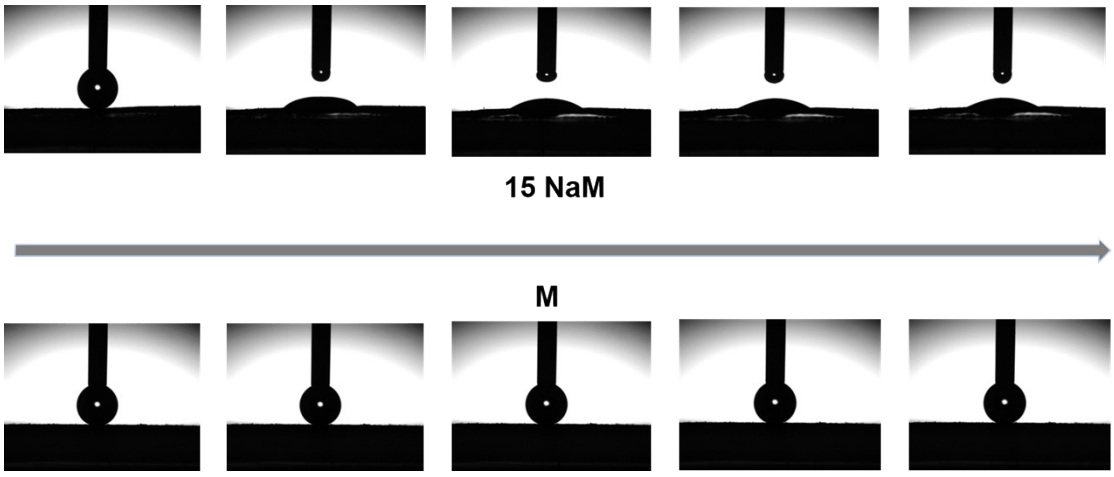

Figure S5. Contact angle experiments for M and 15 NaM were conducted from the initial to the fifth frames depicting the droplet making contact with the catalyst surface.

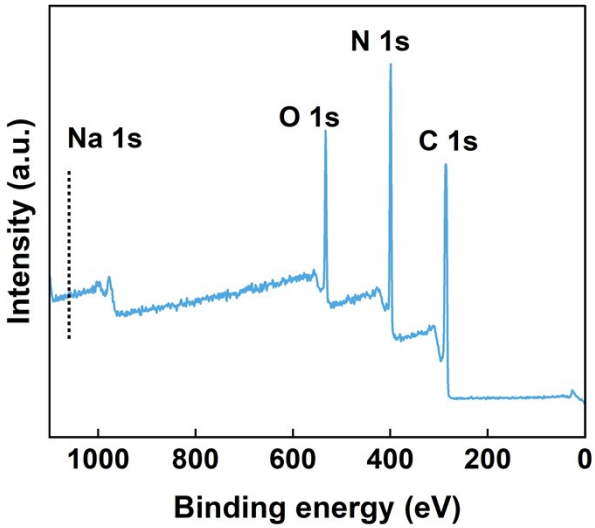

Figure S6. XPS spectra of 15 NaM.

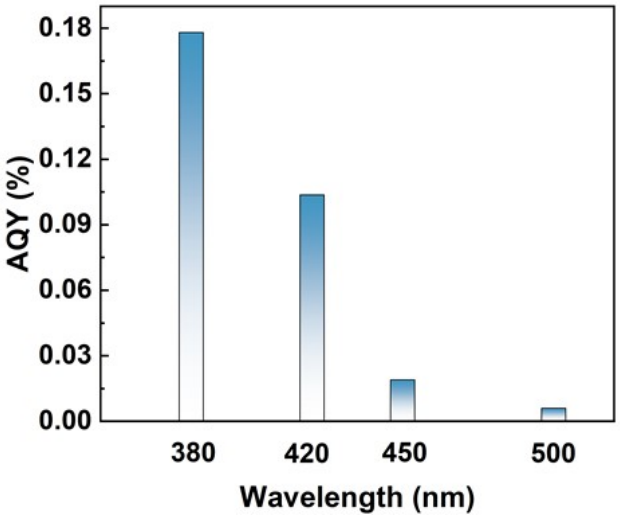

Figure S7. AQY for 15 NaM.

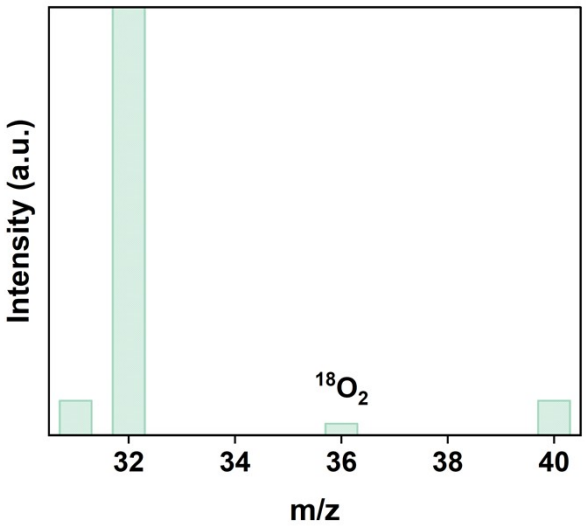

Figure S8. $H_2{}^{18}O$-labeled experiment.

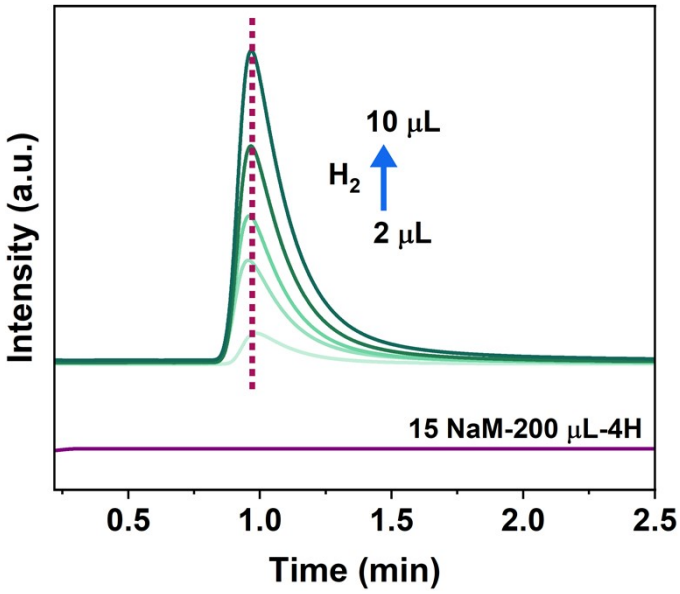

Figure S9. Chromatographic detection profile of H_2.

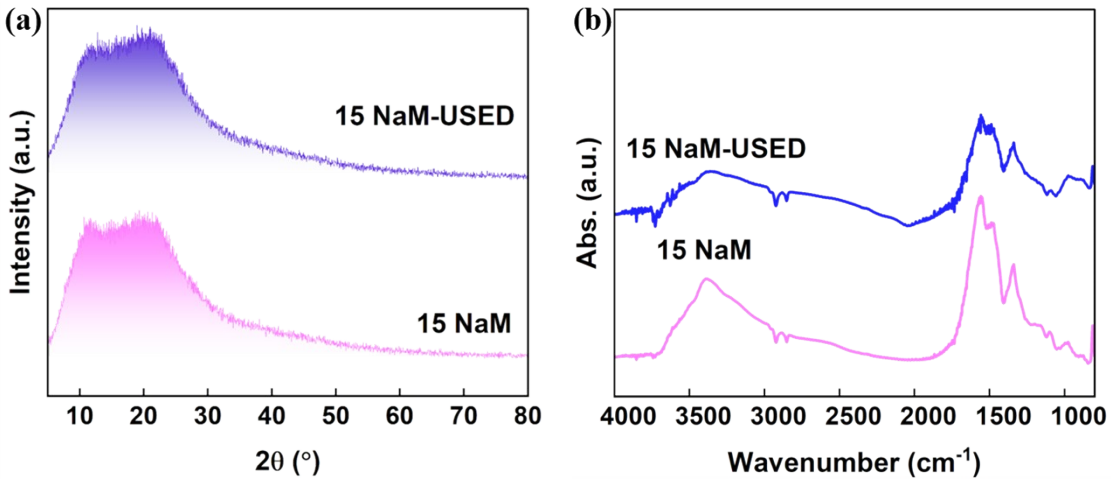

Figure S10. XRD spectra and FT-IR spectra of catalysts after used.

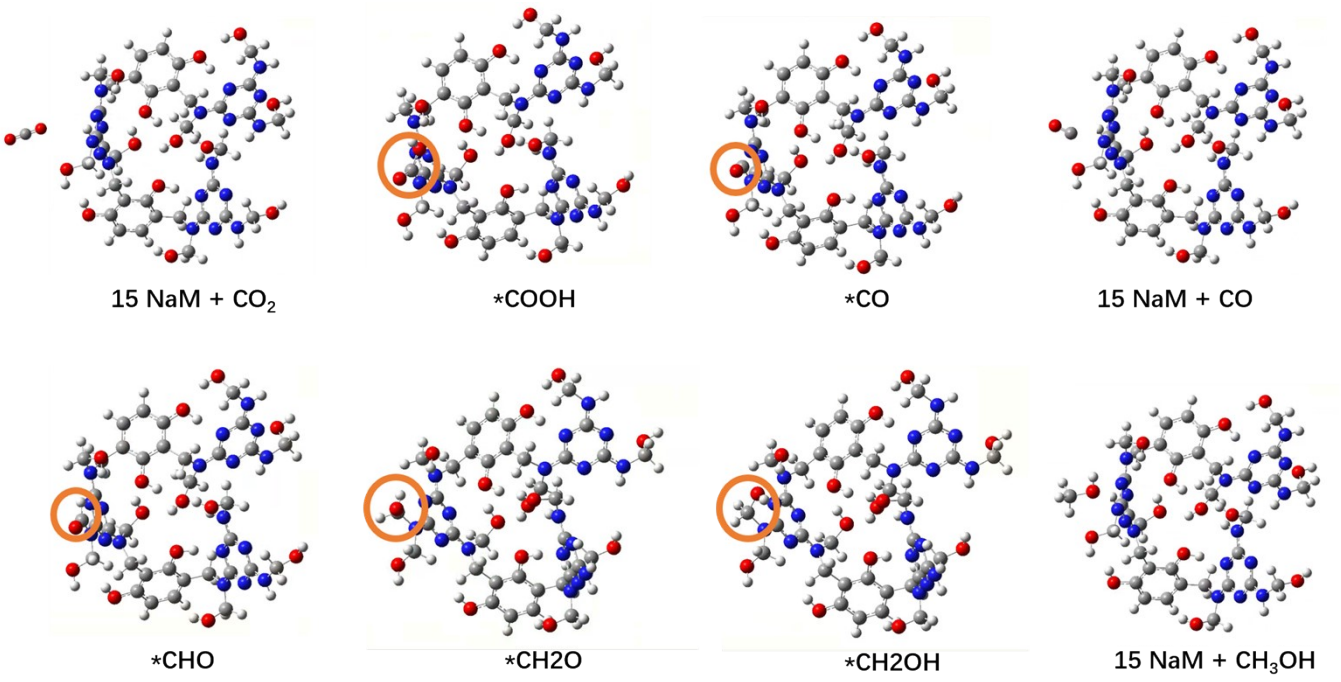

Figure S11. Details of DFT calculations.

References

[1] Z. Fan, X. Li, X. Luo, X. Fei, B. Sun, L. Chen, Z. Shi, C. Sun, X. Shao, H. Zhang, *Advanced Functional Materials* **2017**, *27*, 1702318.

[2] J. Delente, D. Umadevi, S. Shanmugaraju, O. Kotova, G. Watson, T. Gunnlaugsson, *Chemical Communications* **2020**, *56*, 2562-2565.

[3] Wisser, F. M.; Duguet, M.; Perrinet, Q.; Ghosh, A. C.; Alves-Favaro, M.; Mohr, Y.; Lorentz, C.; Quadrelli, E. A.; Palkovits, R.; Farrusseng, D.; Mellot-Draznieks, C.; de Waele, V.; Canivet, J., *Chemie International Edition* **2020**, *59*, 5116-5122.

[4] Piou, T.; Romanov-Michailidis, F.; Ashley, M. A.; Romanova-Michaelides, M.; Rovis, T., *Journal of the American Chemical Society* **2018**, *140*, 9587-9593.

[5] Marenich, A. V.; Cramer, C. J.; Truhlar, D. G. *The Journal of Physical Chemistry B* **2009**, *113*, 6378-6396.

[6] Grimme, S.; Antony, J.; Ehrlich, S.; Krieg, H. *The Journal of Chemical Physics* **2010**, *132*, 154104.

[7] Feng, X., Zheng, R., Gao, C. et al. *Nat Commun* **2022**, *13*, 2146.

[8] Qingqing Lu, Kamel Eid, Wenpeng Li, Aboubakr M. Abdullah, Guobao Xu, Rajender S. Varma *Green Chem*. **2021**,*23*, 5394-5428.

[9] Jun Li, Wenfeng Pan, Qiaoyun Liu*, Zhiquan Chen, Zhijie Chen. *J. Am. Chem. Soc*. **2021**, *143*, 17, 6551–6559.

[10] H. Li; B. Zhu; S. Cao; J. Yu. *Chemical Communications*. **2020**, *56*, 5641-5644.

[11] L. Wang, B. Cheng, L. Zhang, J. Yu. *Small* **2021**, *17*, 2103447.

[12] Soumalya Bhowmik, Shankab J. Phukan, Neeraj K. Sah, Manas Roy, Somenath

Garai, and Parameswar Krishnan Iyer. *ACS Applied Nano Materials.* **2021**, *4*, 12845-12890.

[13] J. Fu; B. Zhu; C. Jiang; B. Cheng; W. You; J. Yu. *Small* **2017**, *13*, 1603938.

[14] Yanghe Fu, Xiaoli Zhu, Liang Huang, Xincong Zhang, Fumin Zhang, *Applied Catalysis B: Environmental* ,**2018**, *239*, 46-51.

[15] J. Fu; B. Zhu; C. Jiang; B. Cheng; W. You; J. Yu. *Small* **2017**, *13* 1603938.

[16] W. Yu, D. Xu and T. Peng, *J. Mater. Chem. A*, **2015**, *3*,19936-19947.